Extremophiles (2012) 16:377–385
DOI 10.1007/s00792-012-0436-1

ORIGINAL PAPER

Effects of the N-terminal and C-terminal domains of *Meiothermus ruber* CBS-01 trehalose synthase on thermostability and activity

Yufan Wang · Jun Zhang · Wenwen Wang · Yanchao Liu · Laijun Xing · Mingchun Li

Received: 13 April 2011 / Accepted: 24 February 2012 / Published online: 9 March 2012

Abstract Numerous trehalose synthases (TreS) from thermophilic microorganisms have extra C-terminal domains. To determine the function of the N- and C-terminal domains of TreS from the thermophilic bacterium *Meiothermus ruber* CBS-01, the two domains were expressed. From the findings, the N-terminal domain from *M. ruber* was not active when compared with that from *Thermus thermophilus*, which had been studied previously. The circular dichroism spectrum showed that the secondary structure of N-terminal domain from *M. ruber* underwent a greater change than that of C terminus. In addition, the N-terminal domain from *T. thermophilus* and C terminus from *M. ruber* were fused. The fusion protein TSTtMr was more efficient and thermostable than the TreS from *M. ruber*. The N-terminal domain from *M. ruber* and C terminus from *T. thermophilus* were fused. The optimum temperature and thermostability of fusion protein TSMrTt were similar to the TreS from *M. ruber*. It was presumed that aside from the C-terminal domain, the N-terminal domain of TreS from thermophilic bacteria could influence thermostability. For the TreS from *M. ruber*, the mutant protein R392F led to a complete loss in activity, and R392A showed a sharp decrease in activity.

Keywords Trehalose · Trehalose synthase (TreS) · *Meiothermus ruber* CBS-01 · *Thermus thermophilus* · N- and C-terminal domains · Thermostability

Communicated by H. Atomi.

Electronic supplementary material The online version of this article (doi:10.1007/s00792-012-0436-1) contains supplementary material, which is available to authorized users.

Y. Wang · W. Wang · Y. Liu · L. Xing · M. Li (✉)
Key Laboratory of Molecular Microbiology and Technology, Department of Microbiology, Nankai University, Ministry of Education, Tianjin 300071, People's Republic of China
e-mail: nklimingchun@yahoo.com.cn

J. Zhang
Tianjin Forestry and Pomology Institute, Tianjin, China

Introduction

Various sugars and sugar alcohols play important roles in the protection of cellular proteins, signal pathways, and energy sources. Among these, trehalose (α-D-glucopyranosyl-1, 1-α-D-glucopyranoside) has attracted extensive interests. Trehalose is a non-reducing disaccharide that has two glucose units linked by α, α-1, 1-glycosidic linkage. It is widely spread throughout bacteria, archaea, yeast, fungi, insects, and plants (Maruta et al. 1996b; Shimakata and Minatagawa 2000; Müller et al. 2001; Elbein et al. 2003; Mahmud et al. 2009). Trehalose has been proven to be an active preservative of proteins, biomasses, pharmaceutical preparations and even organs for transplantation (Schiraldi et al. 2002). Therefore, trehalose is widely used in food, cosmetic, and pharmaceutical industries.

To date, the following five main enzymatic routes involved in trehalose biosynthesis have been discovered: (1) trehalose-6-phosphate synthetase and trehalose-6-phosphate phosphatase (TPS and TPP) (Kaasen et al. 1994), (2) maltooligosyltrehalose trehalohydrolase and maltooligosyltrehalose synthase (TreY and TreZ) (Maruta et al. 1996a), (3) trehalose synthase (TreS) (Nishimoto et al. 1995), (4) trehalose glycosyltransferring synthase (TreT) (Ryu et al. 2005), and (5) trehalose phosphorylase (TreP) (Han et al. 2003).

TreS converts maltose to trehalose in a single step process, which saves time and costs in the industry. Therefore, this enzymatic process shows great advantages and potential in producing trehalose. TreS has been studied to a great extent. It has been cloned from numerous bacteria and archaea (Wei et al. 2004; Lee et al. 2005; Chen et al. 2006; Yue et al. 2009). In addition, the relationship of the structure and function of TreS has also been investigated. TreS from *Mycobacterium smegmatis* has two different binding sites of maltose and trehalose (Pan et al. 2004) and could undergo a self-induced or autocatalytic proteolysis upon long-term storage on ice. TreS also has amylase activity that converts glycogen to trehalose (Pan et al. 2008). In some extremophiles, TreS has an additional C-domain, which may affect the thermophilicity and thermostability of the enzyme (Wang et al. 2007b).

In previous works, the *treS* gene has been cloned from a thermophilic *Meiothermus ruber* strain CBS-01 and expressed in *Escherichia coli* to characterize its properties (Zhu et al. 2008; Zhu et al. 2010). In the present study, the sequence of TreS from *M. ruber* was found to be similar to that from *Thermus thermophilus*. The similarity of the two sequences of N-terminal domain was very high. However, the optimum temperature and thermostability of TreS from the two kinds of organisms were quite different. The N-terminal region of TreS from *T. thermophilus* was active, as observed in a previous work (Wang et al. 2007b), whereas the domain from *M. ruber* was not. This phenomenon attracted the interests of the current researchers in investigating the function of the N- and C-terminal regions of the two enzymes. Thus, a series of truncated *treS* gene expression vectors and fused gene expression vectors were constructed. Kinetic parameters and secondary structures between these recombinant proteins and the wild-type TreS from *M. ruber* strain CBS-01 or *T. thermophilus* HB8 were examined to compare their activities.

Materials and methods

Bacterial strains, plasmids, and reagents

M. ruber CBS-01 (CGMCC1256) and *T. thermophilus* HB8 (ATCC27634) were used in the current study. *E. coli* DH5α and *E. coli* Rosetta-gami (DE3) were from Novagen (Madison, WI) and used as host for the cloning vectors and expression vectors, respectively. Plasmid pET-21a(+) for expression was purchased from Novagen (Novagen, USA). Enzymes for DNA restriction and polymerases for the polymerase chain reaction (PCR) process were from Takara (Takara, China). All saccharides including maltose, trehalose, and glucose were purchased from Sigma (Sigma, USA). The columns used for protein purification were from GE (GE, Sweden). The Amicon Ultra-4 centrifuge was obtained from Millipore (Millipore, USA). The other chemicals and reagents were of analytical grade.

Construction of recombinant expression vectors

The whole *treS* gene (GenBank No. EU443098) of *M. ruber* was amplified from the genomic DNA of *M. ruber* CBS-01 using PCR with primers Ptres-F and Ptres-R (all primers are listed in S1 in Supplementary Material). The open reading frame (ORF) was 2895 bp long. The amplified DNA was ligated into *Eco*RI- and *Sal*I-digested pET-21a(+) to produce pET-TSM. The protein expressed was TSM (Fig. 1a).

The whole *treS* gene (GenBank No. TTHA0478) of *T. thermophilus* was amplified from the genomic DNA of *T. thermophilus* HB8 using PCR with primers PT.t-TreSF and PT.t-TreSR. The ORF was 2898 bp long. The amplified DNA was ligated into the similarly treated pET-21a(+) mentioned above to produce pET-TST. The protein expressed was TST (Fig. 1b).

The TSTtMr fusion protein consisted of 550 amino acids from the N terminus of TST and 412 amino acids from the C terminus of TSM (Fig. 1c). The gene was constructed using overlap PCR. The gene containing the N-terminal fragment of *TST* was cloned with primers PT.t-TreSF and pTtMr1, whereas the gene containing the C-terminal fragment of *TSM* was cloned with primers Ptres-R and pTtMr2. The fusion gene *TSTtMr* was amplified through fusion PCR with primers PT.t-TreSF and Ptres-R. The *TSTtMr* was ligated into *Eco*RI–*Sal* I-digested pET-21a(+) to construct pTSTtMr.

The TSMrTt fusion protein consisted of 540 amino acids from the N terminus of TSM and 423 amino acids from the C terminus of TST (Fig. 1d). The method to construct plasmid pTSMrTt was similar to that of pTSTtMr. The primers for the N-terminal fragment of TSM were Ptres-F and pMrTt1. PT.t-TreSR and pTtMr2 were the primers for the C-terminal fragment of TST. The whole fusion gene was amplified with primers Ptres-F and PT.t-TreSR.

To examine the function of the C-terminal (Fig. 1e) and N-terminal domains (Fig. 1f) of TSM, pET-TSMC and pET-TSMN were constructed. The digested vector pET-21a(+) was ligated with the truncated *treS* gene of *M. ruber* containing 1275 nucleotide residues from C terminus to construct pET-TSMC, and with another truncated gene containing 1650 nucleotide residues from N terminus to construct pET-TSMN. The primers used were pTSC and Ptres-R for *TSMC*, and Ptres-F and pTSN for TSMN.

All the expression vectors were linked with 6 × His-tag at the C terminus to purify with NTA-Ni column.

The recombinant plasmids were transformed into *E. coli* strains Rosetta-gami (DE3) for expression.

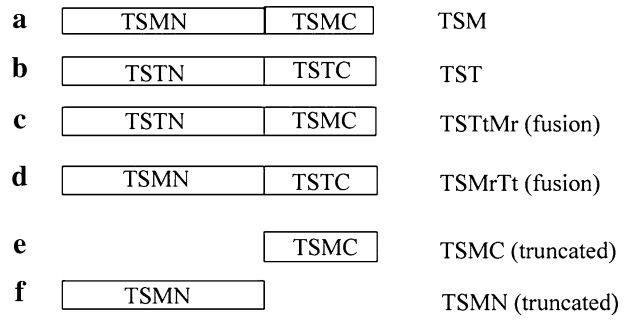

Fig. 1 Expression cassettes of the enzymes TSM, TST, TSTtMr, TSMrTt, TSMC, and TSMN. The recombinant proteins for **a** TSM, **b** TST, **c** TSTtMr: the fusion protein of N-terminal portion of TST (residues 1–550) fused with C-terminal portion of TSM (residues 551–end), **d** TSMrTt: the fusion protein of N-terminal portion of TSM (residues 1–540) fused with C-terminal portion of TST (541aa–end), **e** TSMC: the C-terminal portion of the TreS from *M. rube*r (residues 551–end) and **f** TSMN: the N-terminal portion of the TreS from *M. ruber* (residues 1–550)

Site-directed mutagenesis

The *treS* gene from *M. ruber* in the previously constructed vector pET-TSM was mutated by splicing overlap extension PCR (Warrens et al. 1997).

Expression and purification of recombinant enzymes

The enzymes were expressed and purified using NTA-Ni column chromatography as described previously (Zhu et al. 2010). The pooled enzymes were dialyzed against 10 mM potassium phosphate buffer (pH 6.5). The dialyzed proteins were loaded on a Resource Q column (200 × 10 mm) equilibrated with 10 mM potassium phosphate buffer (pH 6.5). The proteins were eluted with a linear gradient of 0–0.5 M NaCl in the same buffer. The active fractions were pooled, and then the enzyme solution was placed on the Superdex 200 (600 × 10 mm) equilibrated with 10 mM potassium phosphate buffer (pH 6.5). The proteins were eluted with the same buffer at 1 mL/min. The active fractions were pooled, concentrated, and desalted using an Amicon Ultra-4 centrifugal filter. The protein concentration was determined using Bradford's method (Bradford 1976) with BSA as standards or by absorption measurements with extinction coefficients of 1.768, 1.663, 1.784, 1.746, and 1.757 g L^{-1} cm^{-1} at 280 nm for TSM, TSMC, TSMN, R392A, and R392F, respectively.

The purified recombinant enzymes were analyzed in denaturing conditions by sodium dodecyl sulfate-polyacrylamide gel electrophoresis (SDS-PAGE).

Enzyme characterization

The values of k_{cat} and K_m for transformation from maltose to trehalose or trehalose to maltose were determined at optimum temperature in 10 mM potassium phosphate buffer (pH 6.5) for 30 min containing 10–90 mM substrate and 5 μg protein. Lineweaver–Burk plot was used to calculate the values of k_{cat} and K_m.

The optimum temperature of the enzymes was determined by measuring the initial reaction rates over the temperatures ranging from 30 to 75°C with the mixture consisting of 100 mM maltose, 10 mM potassium phosphate buffer (pH 6.5), and 5 μg enzyme for 10 min. The initial rates were determined by fitting experimental data obtained within 10 min to the equation $c = At + B$, where c is the product concentration, t is the time, and A (the initial rate) and B are obtained by linear regression. The half-life of the enzymes at different temperatures was calculated to examine the stability against thermal denaturation. The proteins were incubated at a series of temperatures for various periods of time. The residual activities were then measured. The reaction was terminated by heating at 100°C for 10 min. No product formation was detected using high-performance liquid chromatography (HPLC) at 100°C for the pre-experiment conducted.

The activities of TSMC, TSMN, R392A, and R392F were detected in the 10 mM potassium phosphate buffer (pH 6.5) with 50 mM substrate and 10 μg purified protein after incubation for 2 h at 30 or 50°C. The mixture of TSMC and TSMN of 10 μg each was analyzed in the same conditions as above.

All data were obtained in three parallel tests at least for the properties of the recombinant enzymes.

Analysis of carbohydrate

The quantification of sugars after each enzymatic reaction was carried out using an HPLC system equipped with a differential refractometer detector and a computerized processing unit (Anastar, version 1.1) as previously described (Zhu et al. 2010).

Molecular modeling and analysis

The structural model of TreS from *M. ruber* was based on the reported crystal structure of the catalytic domain of α-glucosidase (PDB code 2ze0) from deep-sea bacterium *Geobacillus* sp. strain HTA-462. The hypothetical conformation was predicted by Swiss-Model Workspace (Arnold et al. 2006; Kiefer et al. 2009) and illustrated as ribbon diagrams using PyMOL. The important functional amino acid residues were predicted following the methods described previously (Song et al. 2007) and support vector machines (SVMs) (Cristianini and Shawe-Taylor 2000; Krishnan and Westhead 2003; Gao et al. 2009) with the assistance of Prof. Tao Zhang from Nankai University.

Circular dichroism (CD) spectroscopy

Circular dichroism spectra were recorded using a MOS-450 Spectrometer (Bio-Logic, USA). Up to 10 μM of each purified protein was used in 10 mM potassium phosphate buffer (pH 6.5) in a 1-mm quartz cell. The spectra were scanned from 190 to 250 nm at a scanning speed of 50 nm/min with a response time of 0.5 s. The data were averaged over three scans.

Results

Sequence analysis of the *treS* gene from *M. ruber* and *T. thermophilus*

The *treS* gene (GenBank No. EU443098) cloned from *M. ruber* genomic DNA (TSM) was 2895 bp long and encoded 964 amino acid residues. Another *treS* gene (GenBank No. TTHA0478) cloned from *T. thermophilus* genomic DNA (TST) was 2898 bp long and encoded 965 amino acid residues. According to a BLAST search, the N-terminal domain from *M. ruber* and *T. thermophilus* shared high similarity with other non-thermophilic TreS, including TreS from *Deinococcus radiodurans* (GenBank No. AE000513), *Myxococcus fulvus* HW-1 (GenBank No. AEI67205), *Stigmatella aurantiaca* DW4/3-1 (GenBank No. YP_003953779.1). The thermostable TreS had an extra C-terminal domain that was missing in other TreS proteins. This domain was reported to play a key role in thermophilicity and thermostability in the TST. In the same study, the N-terminal region (1–550aa) from TST was active (Wang et al. 2007b). TSM was also a thermostable protein from thermophilic *M. ruber*. Through sequence alignment, the identity of the N-terminal domain of TreS between *M. ruber* and *T. thermophilus* was up to 87%, whereas the identity of the C-terminal domain of two proteins was 54% (Fig. 2). Thus, TST and TSM were divided into N-terminal (1–550aa) and C-terminal (551aa–end) domains to analyze their functions.

Construction, expression, and purification of recombinant enzyme

The inserted segments of all the expression vectors were sequenced. Each recombinant enzyme was expressed, purified, and analyzed on SDS-PAGE (10% minigel), which showed a clear protein band. According to previous works, the 6 × His-tag at the C terminus domain did not affect the activity of TreS. Therefore, purified proteins were used in the subsequent study.

Activity of recombinant proteins

The enzymatic activities of two truncated proteins (TSMN and TSMC) and fusion proteins (TSMrTt and TSTtMr) were analyzed by the formation of trehalose on HPLC using maltose as the substrate. No activity of TSMN or TSMC was detected. The mixture was also inactive when these two truncated enzymes were mixed. It could not recover the activity of the wild-type TreS from *M. ruber*. However, the fusion proteins TSMrTt and TSTtMr could convert maltose into trehalose and produce glucose as a byproduct. Similar levels of activity were observed for the reverse reaction catalyzing trehalose to maltose.

Fig. 2 Alignment of the amino acid sequences of trehalose synthases from *M. smegmatis* (GenBank accession number YP_890728), *M. ruber* (GenBank accession number ACA35051), and *T. thermophilus* (GenBank accession number AAQ16097). The putative conserved active sites and substrate-binding sites are denoted by *asterisks*. The mutant site R392 is denoted by *arrowhead*. Residues that are identical are shaded in *gray box*, whereas conserved residues are shaded in *blue box* (color figure online) ▶

Characterization of TSM, TST, TSTtMr, and TSMrTt

Due to fusion proteins, TSMrTt and TSTtMr, displaying the activity to convert maltose into trehalose, kinetic analyses of TSM, TST, TSTtMr, and TSMrTt were performed. The kinetic parameters (K_m and k_{cat}) of TSM, TST, TSMrTt and TSTtMr are given in Table 1.

The K_m values of TSM, TST, and TSMrTt using maltose as substrate were close to that of the three proteins using trehalose as substrate, suggesting that maltose and trehalose were recognized by these proteins with similar affinities. However, the K_m value of TSTtMr using trehalose was about 2.7-fold higher than that of the enzyme using maltose as substrate, which indicated that TSTtMr preferred maltose over trehalose as its substrate. All four proteins displayed higher k_{cat}/K_m values towards maltose than towards trehalose. Among these proteins, TSTtMr displayed the highest value, indicating that it could convert maltose to trehalose more efficiently than the other proteins from a kinetic point of view.

The effects of temperature on the activity and the stability of recombinant enzymes TSM, TST, TSTtMr, and TSMrTt

Figure 3 shows that the optimal temperature of both TSM and TSMrTt was 50°C, whereas the optimal temperature of TST and TSTtMr was 60°C.

Table 2 shows the half-lives of TSM, TST, TSMrTt, and TSTtMr at different temperatures. The half-lives of TSM and TSMrTt were almost the same at 70, 75, and 80°C, which were shorter than those of TST or TSTtMr. Comparing TSTtMr with TST, the half-life of TSTtMr was much shorter than that of TST at 80°C, implying that TST was the most thermostable among the four enzymes.

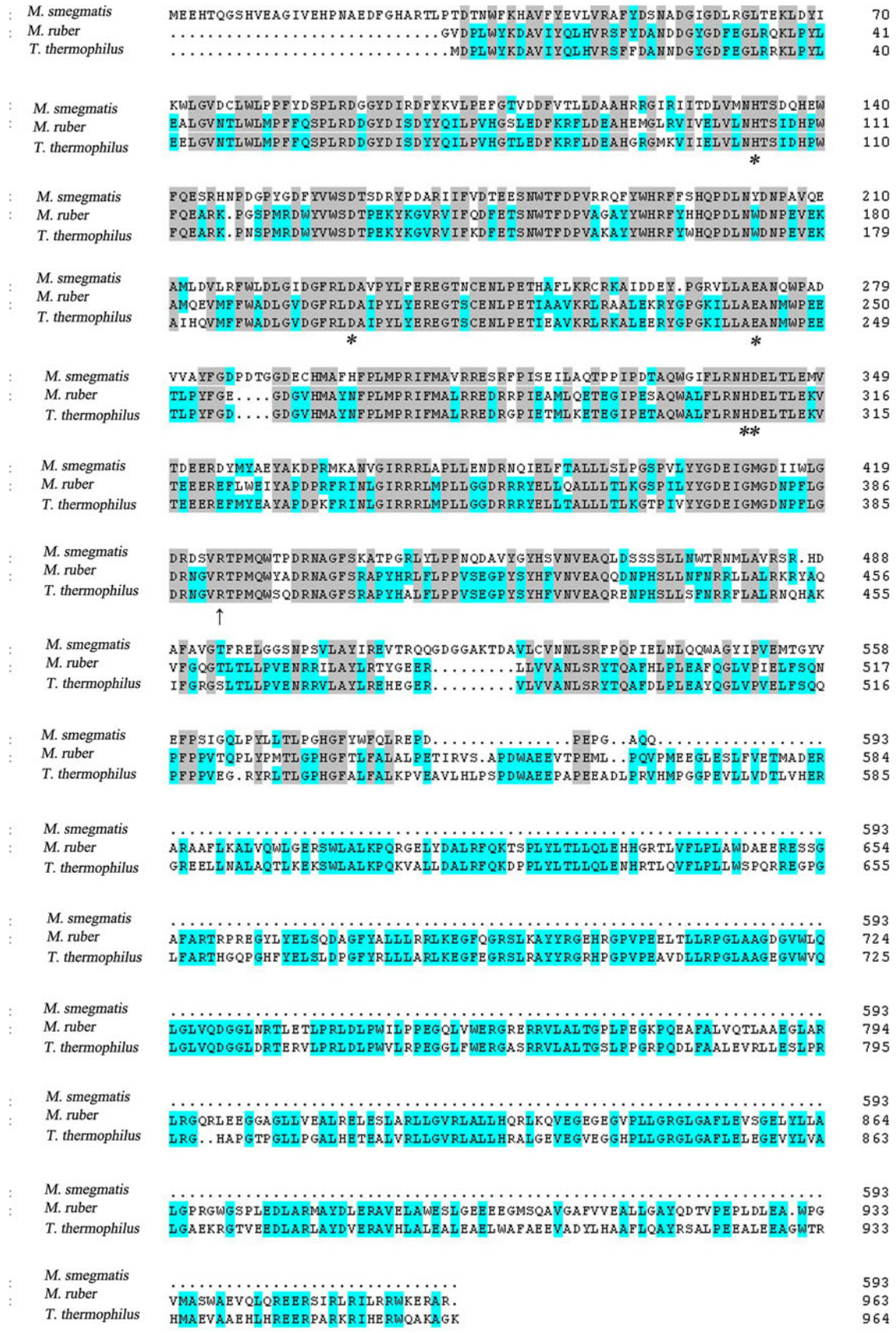
M. smegmatis
M. ruber
T. thermophilus
MEEHTQGSHVEAGIVEHPNAEDFGHARTLPTDTNWFKHAVFYEVLVRAFYDSNADGIGDLRGLTEKLDYI 70
.....GVDPLWYKDAVIYQLHVRSFYDANDDGYGDFEGLRQKLPYL 41
.....MDPLWYKDAVIYQLHVRSFFDANNDGYGDFEGLRRKLPYL 40
KWLGVDCLWLPPFYDSPLRDGGYDIRDFYKVLPEFGTVDDFVTLLDAAHRRGIRIITDLVMNHTSDQHEW 140
EALGVNTLWLMPFFQSPLRDDGYDISDYYQILPVHGSLEDFKRFLDEAHEMGLRVIVELVLNHTSIDHPW 111
EELGVNTLWLMPFFQSPLRDDGYDISDYYQILPVHGTLEDFKRFLDEAHGRGMKVIIELVLNHTSIDHPW 110
FQESRHNPDGPYGDFYVWSDTSDRYPDARIIFVDTEESNWTFDPVRRQFYWHRFFSHQPDLNYDNPAVQE 210
FQEARK.PGSPMRDWYVWSDTPEKYKGVRVIFQDFETSNWTFDPVAGAYYWHRFYHHQPDLNWDNPEVEK 180
FQEARK.PNSPMRDWYVWSDTPEKYKGVRVIFKDFETSNWTFDPVAKAYYWHRFYWHQPDLNWDNPEVEK 179
AMLDVLRFWLDLGIDGFRLDAVPYLFEREGTNCENLPETHAFLKRCRKAIDDEY.PGRVLLAEANQWPAD 279
AMQEVMFFWADLGVDGFRLDAIPYLYEREGTSCENLPETIAAVKRLRAALEKRYGPGKILLAEANMWPEE 250
AIHQVMFFWADLGVDGFRLDAIPYLYEREGTSCENLPETIEAVKRLRKALEERYGPGKILLAEANMWPEE 249
VVAYFGDPDTGGDECHMAFHFPLMPRIFMAVRRESRFPISEILAQTPPIPDTAQWGIFLRNHDELTLEMV 349
TLPYFGE....GDGVHMAYNFPLMPRIFMALRREDRRPIEAMLQETEGIPESAQWALFLRNHDELTLEKV 316
TLPYFGD....GDGVHMAYNFPLMPRIFMALRREDRGPIETMLKETEGIPETAQWALFLRNHDELTLEKV 315
TDEERDYMYAEYAKDPRMKANVGIRRRLAPLLENDRNQIELFTALLLSLPGSPVLYYGDEIGMGDIIWLG 419
TEEEREFLWEIYAPDPRFRINLGIRRRLMPLLGGDRRRYELLQALLLTLKGSPILYYGDEIGMGDNPFLG 386
TEEEREFMYEAYAPDPKFRINLGIRRRLMPLLGGDRRRYELLTALLLTLKGTPIVYYGDEIGMGDNPFLG 385
DRDSVRTPMQWTPDRNAGFSKATPGRLYLPPNQDAVYGYHSVNVEAQLDSSSSLLNWTRNMLAVRSR.HD 488
DRNGVRTPMQWYADRNAGFSRAPYHRLFLPPVSEGPYSYHFVNVEAQQDNPHSLLNFNRRLLALRKRYAQ 456
DRNGVRTPMQWSQDRNAGFSRAPYHALFLPPVSEGPYSYHFVNVEAQRENPHSLLSFNRRFLALRNQHAK 455
AFAVGTFRELGGSNPSVLAYIREVTRQQGDGGAKTDAVLCVNNLSRFPQPIELNLQQWAGYIPVEMTGYV 558
VFGQGTLTLLPVENRRILAYLRTYGEER.....LLVVANLSRYTQAFHLPLEAFQGLVPIELFSQN 517
IFGRGSLTLLPVENRRVLAYLREHEGER.....VLVVANLSRYTQAFDLPLEAYQGLVPVELFSQQ 516
EFPSIGQLPYLLTLPGHGFYWFQLREPD.....PEPG..AQQ..... 593
PFPPVTQPLYPMTLGPHGFTLFALALPETIRVS.APDWAEEVTPEML..PQVPMEEGLESLFVETMADER 584
PFPPVEG.RYRLTLGPHGFALFALKPVEAVLHLPSPDWAEEPAPEEADLPRVHMPGGPEVLLVDTLVHER 585
ARAAFLKALVQWLGERSWLALKPQRGELYDALRFQKTSPLYLTLLQLEHHGRTLVFLPLAWDAEERESSG 654
GREELLNALAQTLKEKSWLALKPQKVALLDALRFQKDPPLYLTLLQLENHRTLQVFLPLLWSPQRREGPG 655
AFARTRPREGYLYELSQDAGFYALLLRRLKEGFQGRSLKAYYRGEHRGPVPEELTLLRPGLAAGDGVWLQ 724
LFARTHGQPGHFYELSLDPGFYRLLLARLKEGFEGRSLRAYYRGRHPGPVPEAVDLLRPGLAAGEGVWVQ 725
LGLVQDGGLNRTLETLPRLDLPWILPPEGQLVWERGRERRVLALTGPLPEGKPQEAFALVQTLAAEGLAR 794
LGLVQDGGLDRTERVLPRLDLPWVLRPEGGLFWERGASRRVLALTGSLPPGRPQDLFAALEVRLLESLPR 795
LRGQRLEEGGAGLLVEALRELESLARLLGVRLALLHQRLKQVEGEGEGVPLLGRGLGAFLEVSGELYLLA 864
LRG..HAPGTPGLLPGALHETEALVRLLGVRLALLHRALGEVEGVEGGHPLLGRGLGAFLELEGEVYLVA 863
LGPRGWGSPLEDLARMAYDLERAVELAWESLGEEEEGMSQAVGAFVVEALLGAYQDTVPEPLDLEA.WPG 933
LGAEKRGTVEEDLARLAYDVERAVHLALEALEAELWAFAEEVADYLHAAFLQAYRSALPEEALEEAGWTR 933
VMASWAEVQLQREERSIRLRILRRWKERAR. 963
HMAEVAAEHLHREERPARKRIHERWQAKAGK 964

Table 1 The kinetic parameters for TSM, TST, TSTtMr, and TSMrTt

	K_m(mM)	k_{cat} (s^{-1})	k_{cat}/K_m (mM^{-1} s^{-1})
Maltose as substrate			
TSM	126 ± 3	147 ± 2	1.16 ± 0.01
TST	97.4 ± 5.9	227 ± 19	2.51 ± 0.05
TSTtMr	57.5 ± 3.0	152 ± 5	2.70 ± 0.03
TSMrTt	79.2 ± 2.3	115 ± 13	1.50 ± 0.06
Trehalose as substrate			
TSM	98.9 ± 1.8	68.9 ± 3.0	0.697 ± 0.008
TST	82.2 ± 3.2	110 ± 11	1.33 ± 0.03
TSTtMr	154 ± 5	202 ± 13	1.32 ± 0.03
TSMrTt	69.6 ± 4.7	61.0 ± 4.3	0.871 ± 0.014

Protein modeling

The three-dimensional structure of the N-terminal domain of TreS from *M. ruber* was predicted at the tertiary level as a GH13 domain (S2 in Supplementary Material). This domain was a catalytic module consisting of 9–543 amino acid residues from N terminus of TSM. Among those, 53 amino acid residues were located in a putative catalytic cleft. H104, D200, H308, and D309, which corresponded to catalytic or substrate-binding residues in other organisms, were in the cleft. It indicated that the predicted cleft may be an important catalytic region.

The activity of mutants of TSM at different temperatures

Support vector machines were used to predict the important functional amino acid residue sites (Cristianini and Shawe-Taylor 2000; Krishnan and Westhead 2003). It predicted protein function changes associated with amino acid substitution using only sequence information, and cross-validated them on a large dataset extracted from the Protein Mutant Database (PMD). By the SVM classifiers, three local sequence features of proteins (residue composition, hydrophobic interaction, and evolutionary property) were investigated (Gao et al. 2009). The algorithm calculated the scores of different amino acid residues at different sites. Larger score represented greater change in the function of protein.

According to the scores, 50 amino acid residues of TSM were recommended for site-directed mutagenesis. We presumed that residues positioned in the putative catalytic cleft would exhibit the largest effects on protein function, and three candidate residues (Y135, F142, and R392) were identified. As R392 was a highly conserved amino acid residue (Fig. 2), it was subjected to site-directed mutagenesis.

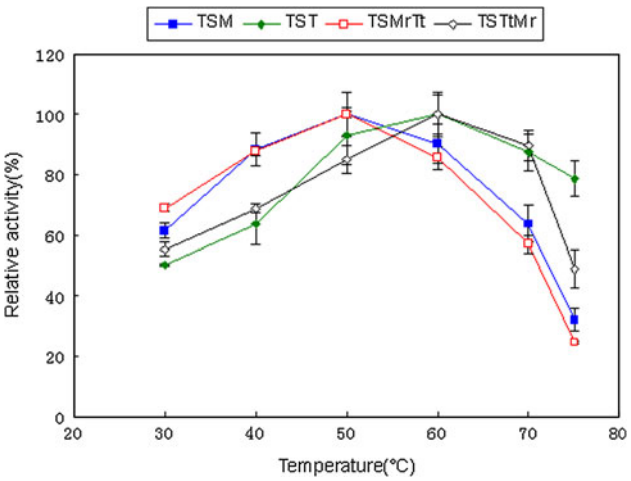

Fig. 3 Effects of temperature on the activity of TSM, TST, TSTtMr, and TSMrTt. The catalytic activity of TSM (*blue*), TST (*green*), TSTtMr (*black*) and TSMrTt (*red*) was assayed at a series of temperatures (30–75°C) (color figure online)

Table 2 The half-lives of the recombinant trehalose synthases

	70°C (min)	75°C (min)	80°C (min)
TSM	48.5 ± 2.7	15.8 ± 2.3	<5
TST	>480	475 ± 5	233 ± 5
TsTtMr	>480	456 ± 3	27.6 ± 3.7
TsMrTt	47.6 ± 2.0	17.6 ± 2.2	<5
TSM(R392A)	42.2 ± 9.4	12.5 ± 4.3	<5

The result of mutagenesis at R392 was predicted by the algorithm based on the signal processing and amino acid sequences (Song et al. 2007; Gao et al. 2009). Initially, R392F with the higher score which indicated greater change in function was chosen to investigate. R392F displayed no activity at different temperatures. Subsequently, R392A with medium score was selected for further examination. R392A was inactive at 50°C and could catalyze maltose into trehalose after being incubated with maltose for 2 h at 30°C. The yield of trehalose was 15.6% of that produced from TSM at 30°C for 30 min. Moreover, the half-life of R392A was a little shorter than that of the wild-type TSM at 70–75°C (Table 2). It indicated that the changes of R392F were greater than that of R392A as predicted.

Secondary structure studies

The far-UV CD spectrum of TSM and TSMC was similar. TSMN did not exhibit an obvious negative or positive peak near three 222, 208 and 195 nm (Fig. 4). The α-helices, β-strands, and random contents were predicted using K2D program (http://www.embl.de/~andrade/k2d.html) (Andrade et al. 1993; Merelo et al. 1994) (data not shown).

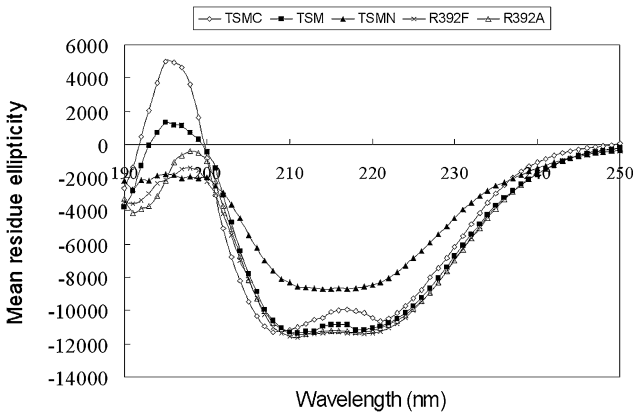

Fig. 4 Far-UV CD spectrum of TSM (*filled squares*), TSMN (*filled triangles*), TSMC (*open squares*), R392F (*crosses*), R392A (*open triangles*)

As shown in Fig. 4, R392F and R392A mutant proteins exhibited similar CD spectra to that of the wild-type TSM, suggesting that the abolishment or decrease in activity of the mutant proteins was not due to dramatic changes in enzyme conformation, but to the residue changes themselves.

Discussion

According to the BLAST search and Swiss-model (http://swissmodel.expasy.org/), the position 9–543 amino acid residues from the N-terminal of TSM belong to the α-amylase family, which shares five conserved amino acid residues and a common $(\alpha/\beta)_8$ barrel structure (MacGregor et al. 2001; Maarel et al. 2002). In this region, 53 amino acid residues were located in a predicted cleft. According to the reaction mechanism and crystal structures of some enzymes belonging to the α-amylase family (MacGregor et al. 2001), the catalytic residues, Asp and Glu, and substrate-binding residues, His, have been deduced and verified in TreS of *Thermus caldophilus* (Koh et al. 2003) and *Picrophilus torridus* (Chen et al. 2006). These residues are conserved in *M. ruber* TreS (Fig. 2). D309 and E243 in TSM are deduced to be involved in catalysis, and H104 and H308 in substrate binding. D200 of TSM was corresponded to D230 of TreS from *M. smegmatis*, which was identified as the nucleophile following a two-step double-displacement catalytic mechanism (Zhang et al. 2011). H104, D200, H308, and D309 were located in the putative cleft. Thus, the cleft in the N-terminal domain was thought to interact with the substrate. However, in contrary to our expectations, TSMN was inactive. In a previous research, the N-terminal of TreS from *T. thermophilus* could convert the reversible reaction of maltose ↔ trehalose (Wang et al. 2007b). However, as shown in Fig. 2, TSMN was inactive because of the 11.7% differences between the two sequences. Subsequently, the protein TSMC without the N-terminal domain was constructed to detect the function of the C-terminal domain of TreS. After mixing TSMN and TSMC, the conversion of maltose into trehalose could not be retrieved. These two parts could not process the reaction separately, implying that unlike TST, the integrity of the structure or the C-terminal domain may be more significant to the function of TSM.

CD spectroscopy was utilized to analyze the secondary structure and classify the tertiary structure of the two truncated proteins and wild-type TSM. TSMN contained more α-helices and lesser β-strands than TSM (data not shown). As displayed in Fig. 4, TSM was primarily an α/β protein (Greenfield 1996). TSMN did not show a clear peak near the 222, 208 and 195 nm, which indicated that the structure of TSMN was impaired. So the N-terminal portion of TSM without the C-terminal domain could not fold as TSM did. Although TSMN contained five conserved amino acid residues of the α-amylase family and a predicted active cleft, the conformation may be impaired, leading to the loss in activity. This observation indicated that the C-terminal domain was important to the structure.

The extra C-terminal domain of TreS from *T. thermophilus* was reported to play a key role in thermophilicity and thermostability (Wang et al. 2007b). Although there was not so much difference between the sequences of TSM and TST, the kinetic parameters, thermophilicity and thermostability of the two proteins differed greatly. The foregoing was the reason why TreS from *T. thermophilus* was chosen for constructing the fusion proteins. The N-terminal and C-terminal domains of TSM and TST were switched to ascertain which of them played the important role in the characteristics and function of TreS. Two recombinant proteins, namely, TSTtMr and TSMrTt, were constructed. At 70 or 75°C, the half-lives of TST and TSTtMr were longer than that of the protein missing a C-terminal domain from *T. thermophilus* (the half-life was less than 1 h). This finding proved that the extra C-terminal domain from the thermophilic TreS could preserve the thermostability of enzyme. In addition, the protein from *M. ruber* without C-terminal domain was inactive. However, the fusion enzyme TSMrTt recovered the activity. Although the sequences of the C-terminal region extensively differed, the fusion proteins TSMrTt and TSTtMr were both active, implying that the C-terminal region may contribute to the activity of the protein.

For TSM, TSMrTt, TST, and TSTtMr, the proteins had the same optimum temperature and similar half-lives if they possessed the same N-terminal domain. The fusion of different C-terminal regions did not significantly alter the optimum temperatures or their half-lives, implying that the N-terminal domains themselves also play a major role in

determining the thermostability and optimum temperature of enzymes.

In some cases, the fusion of multiple enzymes provides physical proximity between the catalytic sites of the individual enzymes, enabling the reactions to be carried out more efficiently (Seo et al. 2000; Wang et al. 2007a; Seo et al. 2008). In the current study, the fusion protein TSTtMr showed some advantages in catalytic efficiency. Comparing their k_{cat}/K_m values, that of TSTtMr was greater than the k_{cat}/K_m value of wild-type TST or TSM using maltose as substrate. Thus, TSTtMr could convert maltose to trehalose faster and was stable at high temperatures. Although the half-life of TsTtMr at 80°C was shorter than that of TST, high temperature is unnecessary in the industry. These two points make TSTtMr suitable for use in the production of trehalose in the industry.

R392A showed a lower reaction temperature and a little shorter half-life at 70–75°C than TSM. There were many factors and mechanisms of protein thermostabilization, including ionic interaction, hydrophobic interaction, hydrogen bonds, etc. (Fessas et al. 2007; Scirè et al. 2008). The crystal structure of TreS had not been reported yet. Thus, the mechanisms of its thermostabilization could not be made clear. However, this phenomenon provided a potential region for the investigation of the activity and thermostability of TreS.

Acknowledgments The authors would like thank Professors Tao Zhang and Jiafu Long from Nankai University for their assistance in this research. The current work was supported by the Tianjin Natural Science Foundation (No. 10JCYBJC09600, 10JCYBJC05000) and the National Natural Science Foundation of China (No. 21076162).

References

Andrade MA, Chacón P, Merelo JJ, Morán F (1993) Evaluation of secondary structure of proteins from UV circular dichroism using an unsupervised learning neural network. Prot Eng 6:383–390

Arnold K, Bordoli L, Kopp J, Schwede T (2006) The Swiss-Model Workspace: a web-based environment for protein structure homology modeling. Bioinformatics 22:195–201

Bradford MM (1976) A rapid and sensitive method for the quantitation of microgram quantities of protein utilizing the principle of protein-dye binding. Anal Biochem 72:248–254

Chen YS, Lee GC, Shaw JF (2006) Gene cloning, expression, and biochemical characterization of a recombinant trehalose synthase from *Picrophilus torridus* in *Escherichia coli*. J Agric Food Chem 54:7098–8104

Cristianini N, Shawe-Taylor J (2000) An introduction to support vector machines and other kernel-based learning methods. Cambridge University Press, Cambridge

Elbein AD, Pan YT, Pastuszak I, Carroll D (2003) New insights on trehalose: a multifunctional molecule. Glycobiol 13:17–27

Fessas D, Staiano M, Barbiroli A, Marabotti A, Schiraldi A, Varriale A, Rossi M, D'Auria S (2007) Molecular adaptation strategies to high temperature and thermal denaturation mechanism of the D-trehalose/D-maltose-binding protein from the hyperthermophilic archaeon *Thermococcus litoralis*. Proteins 67:1002–1009

Gao S, Zhang N, Duan GY, Yang Z, Ruan JS, Zhang T (2009) Prediction of function changes associated with single-point protein mutations using support vector machines (SVMs). Hum Mutat 30:1161–1166

Greenfield NJ (1996) Methods to estimate the conformation of proteins and polypeptides from circular dichroism data. Anal Biochem 235:1–10

Han SE, Kwon HB, Lee SB, Yi BY, Murayama I, Kitamoto Y, Byun MO (2003) Cloning and characterization of a gene encoding trehalose phosphorylase (TP) from *Pleurotus sajor-caju*. Protein Expr Purif 30:194–202

Kaasen I, McDougall J, StroØm AR (1994) Analysis of the otsBA operon for osmoregulatory trehalose synthesis in *Escherichia coli* and homology of the OtsA and OtsB proteins to the yeast trehalose-6-phosphate synthase/phosphatase complex. Gene 145:9–15

Kiefer F, Arnold K, Künzli M, Bordoli L, Schwede T (2009) The Swiss-model Repository and associated resources. Nucleic Acids Res 37:D387–D392

Koh S, Kim J, Shin HJ, Lee D, Bae J, Kim D, Lee DS (2003) Mechanistic study of the intramolecular conversion of maltose to trehalose by *Thermus caldophilus* GK24 trehalose synthase. Carbohydr Res 338:1339–1343

Krishnan VG, Westhead DR (2003) A comparative study of machine-learning methods to predict the effects of single nucleotide polymorphisms on protein function. Bioinformatics 19:2199–2209

Lee JH, Lee KH, Kim CG, Lee SY, Kim GJ, Park YH, Chung SO (2005) Cloning and expression of a trehalose synthase from *Pseudomonas stutzeri* Cj38 in *Escherichia coli* for the production of trehalose. Appl Microbiol Biotechnol 68:213–219

MacGregor EA, Janecek S, Svensson B (2001) Relationship of sequence and strcture to specificity in the alpha-amylase family of enzymes. Biochim Biophys Acta 1546:1–20

Mahmud SA, Nagahisa K, Hirasawa T, Yoshikawa K, Ashitani K, Shimizu H (2009) Effect of trehalose accumulation on response to saline stress in *Saccharomyces cerevisiae*. Yeast 26:17–30

Maruta K, Hattori K, Nakada T, Kubota M, Sugimoto T, Kurimoto M (1996a) Cloning and sequencing of trehalose biosynthesis genes from *Arthrobacter* sp. Q36. Biochim Biophys Acta 1289:10–13

Maruta K, Hattori K, Nakada T, Kubota M, Sugimoto T, Kurimoto M (1996b) Cloning and sequencing of trehalose biosynthesis genes from *Rhizobium* sp. M-11. Biosci Biotechnol Biochem 60:717–720

Merelo JJ, Andrade MA, Prieto A, Morán F (1994) Proteinotopic feature maps. Neurocomputing 6:443–454

Müller J, Aeschbacher RA, Wingler A, Boller T, Wiemken A (2001) Trehalose and trehalase in *Arabidopsis*. Plant Physiol 125:1086–1093

Nishimoto T, Nakano M, Bnakada T, Chaen H, Fukuda S, Sugimoto Y, Kurimoto M, Tsujisaka Y (1995) Purification and properties of a novel enzyme, trehalose synthase, from *Pimelobacter* sp. R48. Biosci Biotechnol Biochem 60:640–644

Pan YT, Edavana VK, Jourdian WJ, Edmondson R, Carroll JD, Pastuszak I, Elbein AD (2004) Trehalose synthase of *Mycobacterium smegmatis*: purification, cloning, expression, and properties of the enzyme. Eur J Biochem 271:4259–4269

Pan YT, Carroll JD, Asano N, Pastuszak I, Edavana VK, Elbein AD (2008) Trehalose synthase converts glycogen to trehalose. FEBS J 275:3408–3420

Ryu SI, Park CS, Cha J, Woo EJ, Lee SB (2005) A novel trehalose-synthesizing glycosyltransferase from *Pyrococcus horikoshii*: molecular cloning and characterization. Biochem Biophys Res Commun 329:429–436

Schiraldi C, di Lernia I, de Rosa M (2002) Trehalose production:exploiting novel approach. Trends in Biotechnol 20:420–425

Scirè A, Marabotti A, Aurillia V, Staiano M, Ringhieri P, Ioaaino L, Crescenzo R, Tanfani F, D'Auria S (2008) Molecular strategies for protein stabilization: the case of a trehalose/maltose-binding protein from *Thermus thermophilus*. Proteins 73:839–850

Seo HS, Koo YJ, Lim JY, Song JT, Kim CH, Kim JK, Lee JS, Choi YD (2000) Characterization of a bifunctional enzyme fusion of trehalose-6-phosphate synthetase and trehalose-6-phosphate phosphatase of *Escherichia coli*. Appl Environ Microbiol 66:2484–2490

Seo JS, An JH, Cheong JJ, Choi YD, Kim CH (2008) Bifunctional recombinant fusing enzyme between maltooligosyltrehalose synthase and maltooligosyltrehalose trehalohydrolase of thermophilic microorganism *Metallosphaera hakonensis*. J Microbiol Biotechnol 18:1544–1549

Shimakata T, Minatagawa Y (2000) Essential role of trehalose in the synthesis and subsequent metabolism of corynomycolic acid in *Corynebacterium matruchotii*. Arch Biochem Biophys 380:331–338

Song Z, Zhang N, Ruan J-s, Yang Z, Zhang T (2007) Prediction of functional point mutants of proteins based on the amino acid sequences. Acta Biophys Sinica (in Chinese) 23:134–138

van der Maarel MJ, van der Veen B, Uitdehaag JC, Leemhuis H, Dijkhuizen L (2002) Properties and applications of starch-converting enzymes of the alpha-amylase family. J Biotechnol 94:137–155

Wang JH, Tsai MY, Lee GC, Shaw JF (2007a) Construction of a recombinant thermostable beta-amylase-trehalose synthase bifunctional enzyme for facilitating the conversion of starch to trehalsoe. J Agric Food Chem 55:1256–1263

Wang JH, Tsai MY, Chen JJ, Lee GC, Shaw JF (2007b) Role of the C-terminal domain of T*hermus thermophilus* trehalose synthase in the thermophilicity, thermostability, and efficient production of trehalose. J Agric Food Chem 55:3435–3443

Warrens AN, Jones MD, Lechler RI (1997) Slicing by overlap extension by PCR using asymmetric amplification: an improved technique for the generation of hybrid proteins of immunological interest. Gene 186:29–35

Wei YT, Zhu QX, Luo ZF, Lu FS, Chen FZ, Wang QY, Huang K, Meng JZ, Wang R, Huang RB (2004) Cloning, expression and identification of a new trehalose synthase gene from *Thermobifida fusca* genome. Acta Biochim Biophys Sinica 36:477–484

Yue M, Wu XL, Gong WN, Ding HB (2009) Molecular cloning and expression of a novel trehalose synthase gene from *Enterobacter hormaechei*. Microb Cell Fact 8:34

Zhang R, Pan YT, He S, Lam M, Brayer GD, Elbein AD, Withers SG (2011) Mechanistic analysis of trehalose synthase from *Mycobacterium smegmatis*. J Biol Chem 286:35601–35609

Zhu Y, Zhang J, Wei D, Wang Y, Chen X, Xing L, Li M (2008) Isolation and Identification of a thermophilic strain producing trehalsoe synthase from geothermal water in China. Biosci Biotechnol Biochem 72:019–2024

Zhu Y, Wei D, Zhang J, Wang Y, Xu H, Xing L, Li M (2010) Overexpression and characterization of a thermostable trehalose synthase from *Meiothermus ruber*. Extremophiles 14:1–8